Fe^{3+} as near-infrared luminescence center in ZnS

A. Hoffmann, R. Heitz, and I. Broser
Institut für Festkörperphysik, Technische Universität Berlin, Hardenbergstrasse 36, D-1000 Berlin 12, Germany
(Received 19 July 1989)

A richly structured luminescence is observed in the 1.2-μm spectral region in "pure" and Fe-doped ZnS crystals for the first time. By means of emission, excitation, and magneto-optical measurements an unambiguous assignment to the $^4T_1(G)$-$^6A_1(S)$ transition of isolated Fe^{3+} on Zn^{2+} lattice sites becomes possible. Basic arguments are the sixfold degeneracy of the ground state with an isotropic g factor of 2.026 ± 0.010, the long decay time of about 4 ms, and the influence of additional iron doping. The excitation mechanism can be described by an energy transfer via free holes from Cu^{2+} to Fe^{2+} centers and a charge-transfer process $Fe^{3+}\xrightarrow{h\nu}Fe^{2+}+h_{VB}$ (VB denotes valence band). A comparison with the well-known isoelectronic Mn^{2+} centers reveals striking similarities. The numerous zero-phonon lines at $T=1.8$ K are due to the polytypic structure of the investigated crystals, offering several different Zn^{2+} lattice sites. The observed fine structures of the $^4T_1(G)$ terms and their behavior in a magnetic field indicate a strong Jahn-Teller coupling to E modes as is known for the Mn^{2+} centers.

I. INTRODUCTION

In most semiconductors $3d$ transition elements are well known as deep centers which strongly influence their electrical[1] and optical[2] properties. There are numerous reasons for the great importance of the transition-metal defects. They are unintentionally contaminated in II-VI compound semiconductors acting even in "high-purity" examples as very effective deep traps for free carriers due to their ability to occupy different charge states.[3] The open-shell configuration of the transition-metal impurities is normally connected with several localized deep levels in the forbidden gap.[4] The multistep transition between these deep levels is a characteristic property of the deep defect and often creates a quenching of the visible luminescence[5] of the specimen. Thus, knowledge of the structure and optical properties of deep centers from $3d$ elements is a prerequisite for a detailed understanding of the electrical and optical behavior of semiconductors.

A common contamination found in II-VI compound semiconductors and, in particular, in ZnS is iron, which is known to quench the visible photoluminescence. Iron prefers to occupy cation lattice sites in the isoelectronic (neutral) charge state[6] but can also accept the two charge states[7] Fe^{1+} and Fe^{3+} or form associates with other point defects such as copper or silver. The charge-transfer processes between these charge states have been studied by photoelectron-spin-resonance (ESR) measurements.[8] Information about the inner structure of the isoelectronic Fe^{2+} has been obtained from optical[9] and optically detected magnetic resonance (ODMR) (Ref. 10) measurements, i.e., the infrared luminescence processes originating from the $^3T_1(H)$-$^5E(D)$ and $^5T_2(D)$-$^5E(D)$ transitions have been observed in ZnS.

In the 1.2-μm near-infrared spectral region in literature[11–13] several structureless luminescence bands have been reported for ZnS crystals. Although many experimental efforts have been made, in most cases no clear identification of their origin has been possible.

In this paper we shall report on a richly structured luminescence in the near-infrared spectral region. The magneto-optical, excitation, and crystal chemical behavior allow us to demonstrate without doubt that it originates from an $Fe^{3+}(^4T_1(G)$-$^6A_1(S))$ transition. Analogies to the well-known case of Mn^{2+} in ZnS, which also has the d^5 configuration, will be discussed.

II. EXPERIMENTAL METHODS

The crystals were high-quality bulk specimens with dimensions in the millimeter range grown by Dr. R. Broser (Fritz-Haber-Institut, Max-Planck-Gesellschaft, Berlin, and collaborators). The crystals have a preferably cubic structure with stacking faults and have subsequently been doped with Cu, Ni, or Fe with concentrations in the sub-ppm range. A detailed description of crystals and the principles of the doping procedure can be found in Ref. 14. The samples were immersed in liquid He at temperatures around 1.8 K and, for measurements at higher temperatures, in a continuous He flow of variable temperature.

Photoluminescence was excited with the 488-nm emission of a 2-W Ar^+-ion laser (Spectra Physics). Light from the crystals has been decomposed in a 0.75-m double-grated monochromator (Spex Industries) and detected with a liquid-N_2-cooled Ge photodiode (North Coast EO817L), using a lock-in technique by chopping the exciting light with 80 Hz. The experiments in a magnetic field have been carried out using a 15-T superconducting magnet built according to the split-coil technique (Intermagnetics and Janis, Inc.). The decay measurements were performed with the same setup as the photoluminescence measurements, but a faster Ge photodiode (North Coast EO817P) in connection with a boxcar averager was used.

was used.

The excitation spectra were measured using a combination of a 0.75-m double-grated monochromator with two gratings ($\lambda_{blaz}=1.6$ μm or 500 nm) and a xenon or halogen lamp as high-resolution tunable light source. The different near-infrared emissions were detected by a double-prism monochromator (Zeiss MM12), which, in addition, allowed us to control the emission spectra. All spectra were corrected for the apparative responses.

III. EXPERIMENTAL RESULTS

Despite the different doping procedures by diffusion of Cu, Ni, or Fe into the specimens, the investigated ZnS crystals show very similar near-infrared emission spectra, with well-known structures. Figure 1 represents a typical spectrum under 488-nm excitation. All spectra are dominated by the extensively investigated $^2E(D)$-$^2T_2(D)$ luminescence of isolated Cu^{2+} around 1.5 μm (Refs. 15 and 16) and show a broad luminescence band around 1.0 μm, which recently has been attributed to the spin-forbidden $^3T_1(H)$-$^5E(D)$ transition of isolated[9] or Cu-associated[10] Fe^{2+}. In better-resolved spectra, the zero-phonon line doublet, first observed by Skowronsky *et al.*[9] for isolated Fe^{2+}, is observable, indicating the presence of isolated iron centers in the investigated crystals. In the spectral region between 800 and 900 nm, we observe an overlap of the $Ni^{2+}(^3T_1(P)$-$^3T_1(F))$ luminescence[17,18] and the M band,[19,20] whereby their intensity ratio depends strongly on the Ni content. The unknown weak luminescence in the 1.40-μm spectral region with zero-phonon lines at 0.9000 eV is, up to now, unknown but will be represented in more detail in Ref. 21. The purpose of the present work is to present detailed investigations of the new, richly structured, luminescence spectra around 1.25 μm, which is very common in our crystals. Figure 2 shows the new luminescence structure around 1.25 μm over an enlarged energy scale. The spectrum begins with a group of sharp emission lines in the energy range between 1.013 and 1.027 eV (see Fig. 3). Due to their small half-width ($\approx$200 μeV) and their location on the high-energy side of the luminescence, we interpret them as zero-phonon lines, possibly connected with the same electronic transition of defects on crystallographic different lattice sites ($T=1.8$ K). The emissions are arranged in three closely spaced groups around 1.015, 1.018, and 1.026 eV and labeled AN, PN, and AS, respectively, according to the different environments of the centers. The dominant intense emission AN at 1.013 99 eV is assumed to be due to the pure cubic center, because of the predominant cubic structure of the investigated crystals. The numerous closely spaced emissions create difficulties to identify the corresponding components in a magnetic field or at higher temperatures ($T>1.8$ K), but the dominating intensity of the AN emission makes it possible to separate their components. In the following

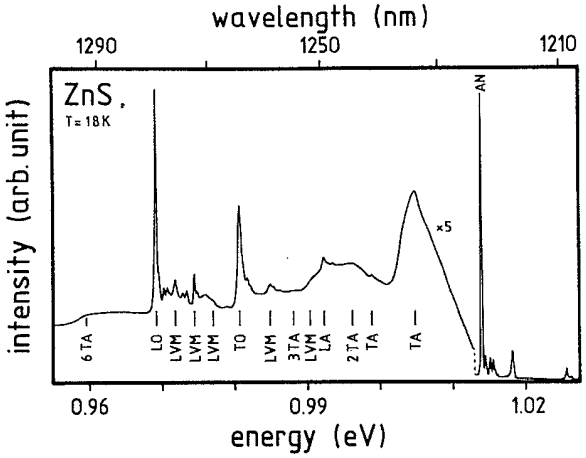

FIG. 2. The same luminescence as in Fig. 1; spectrum of a polytypic ZnS crystal in the 1.25-μm spectral range. Only the emission lines of the cubic AN center are marked.

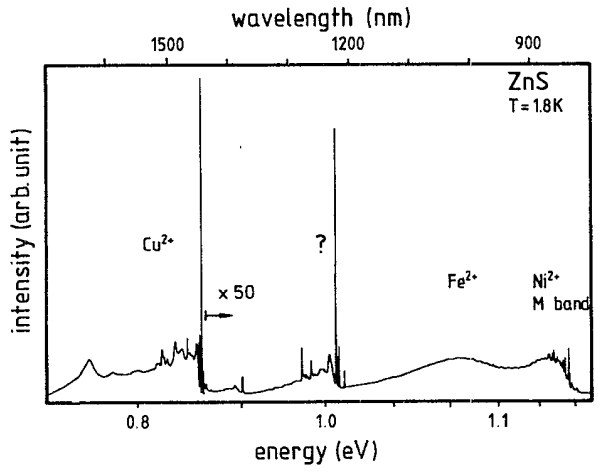

FIG. 1. Luminescence spectrum of ZnS in the near-infrared spectral region, taken under excitation with light of the 488-nm emission of an Ar^+-ion laser.

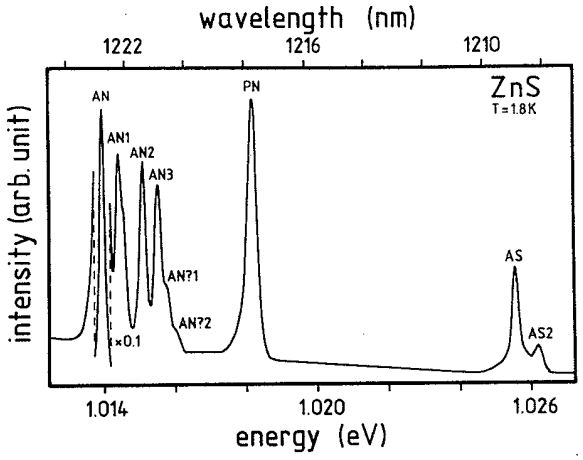

FIG. 3. Zero phonon lines of the new luminescence in an enlarged energy scale. AN, cubic; PN and AS, stacking faults.

we will report mainly the results of the cubic AN center and take the AN emission as reference for the polytypic emissions. The energy positions and proposed interpretations of the zero-phonon lines are summarized in Table I.

On the low-energy side of the zero-phonon region, we observe a weak but complicated phonon-assisted spectrum (see Fig. 2). The relatively strong broad underground results from the coupling to phonons with an energy of 9.2 meV. We can trace up to nine phonon sidebands with decreasing intensities. The phonon energy corresponds well to the TA(L) mode of the host lattice.[22] Two intense phonon sidebands appear at energies below the AN emission shifted 33.3 and 44.9 meV, respectively. These energies are close to those of the fundamental optical modes TO (33.8 meV) and LO (43.6 meV) observed in Raman spectra[23] or by the investigation of the far-infrared dielectric function.[24] Special attention should be given to the small full width at half maximum (FWHM) from the AN–LO-phonon sideband of 270 μeV. In the range between the TA(L) and TO phonons three further phonons with energy shifts of 15.3, 21.7, and 29.1 meV occur. The first two of them are situated in the acoustical branch of the host lattice, whereas the phonon mode with 29.1 meV lies in the gap between the optical and acoustical branch. This mode is an impurity-induced gap mode.

In addition to the fundamental modes, three further phonons with energies of 36.8, 39.5, and 42.2 meV occur in the optical-phonon range. These energies correspond to those of the optical host phonons on different distinct points of the Brillouin zone. On the other hand, Zigone *et al.*[25] observed very similar phonons in Raman spectra of transition-metal doped ZnS (see Table II for ZnS:Fe), which they explained as impurity modes. In general it is obvious that the phonon coupling to the ground state of the new luminescence is very weak, due to the lack of two phonon sidebands, except for the TA(L) phonon. The observed phonon energies and their interpretations are summarized in Table II. In Fig. 2, only the phonon sidebands of the cubic AN center are marked. The distorted centers show the same phonon sidebands shifted to higher energies according to the separations of the zero-phonon lines. Though the emissions of the polytypic centers should be polarized in accordance with the observations for the polytypic Cu^{2+} and Ni^{2+} centers in the investigated crystals, we did not observe any polarization effects for the new luminescence centers.

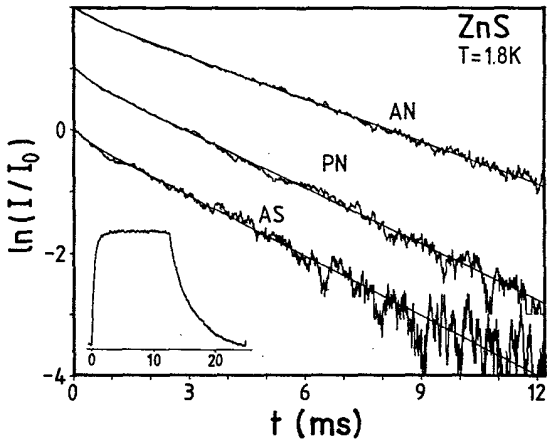

FIG. 4. The decay of the AN, PN, and AS luminescence bands under quasi-dc excitation with a chopped Ar-ion laser (τ_{AN}=4.3 ms, τ_{PN}=3.3 ms, τ_{AS}=3.1 ms).

An important feature of the new luminescence is the long lifetime of the excited state in the order of some ms and it should be noted that with increasing excitation intensity the luminescence can be saturated. Figure 4 represents the decay of the new luminescence under quasi-dc excitation with a chopped Ar-ion laser. The energy resolution of the detecting system (ΔE =2 meV) allows us to separate the AN, PN, and AS emissions. A monoexponential decay can be seen with 4.3±0.2 ms for the AN center. In contrast to this the PN and AS centers show shorter decay times of 3.3±0.2 ms and 3.1±0.2 ms. These relatively long decay times indicate that spin-forbidden transitions are involved for the luminescence process. Absorption measurements in the near-infrared spectral region reveal the $Ni^{2+}(^3T_1(F)$-$^3T_1(P))$ (Ref. 17) and $Cu^{2+}(^2T_2(D)$-$^2E(D))$ (Ref. 15) transitions, but we

TABLE I. The observed zero-phonon energies of the $^4T_1(G)$-$^6A_1(S)$ transitions at T=1.8 K and the observed splittings of the $^4T_1(G)$ terms for the polytypic Fe^{3+} centers.

Center	E_{NPL} (eV)	FWHM (μeV)	$E-E$(AN) (meV)	$\Delta E(^4T_1(G))$ (meV)
AS2	1.026 21		12.22	0.77
AS	1.025 62	250	11.63	0.48
AS?	1.025 06		11.07	
PN	1.018 23	300	4.24	0.86,1.72,2.75
PN?	1.017 62		3.63	
AN?	1.016 13		2.14	
AN?	1.015 86		1.87	
AN3	1.015 56	220	1.57	1.45
AN2	1.015 13	210	1.14	1.31
AN1	1.014 45	220	0.58	
AN	1.013 99	180		0.58

TABLE II. The observed phonon energies and their interpretations. In addition, the impurity-induced modes observed by Zigone *et al.* (Ref. 25) for ZnS:Fe are presented. LVM denotes local vibrational mode.

hw observed (meV)	Interpretation	hw(Fe)[a] (meV)
9.2±0.2	TA(L)	
15.3±0.2	TA	
21.7±0.1	LA	
23.7±0.1	LVM	
29.1±0.1	LVM	
33.3±0.1	TO	
36.8±0.1	LVM	37.1
		38.4
39.5±0.1	LVM	40.7
		41.2
42.2±0.1	LVM	42.0
44.9±0.1	LO	

[a] Reference 25.

have failed to detect any absorptions correlated to the luminescence in question. The lack of absorption can be due to the small absorption cross section corresponding to the observed long decay time or the absence of luminescence centers in the unexcited crystals. This will be discussed later.

In order to understand the origin of the new luminescence we undertook magneto-optical measurements for various orientations of the crystals in magnetic fields up to 15 T. The very complex spectra can be explained by identical splittings of each emission line. Figure 5 shows the clearly resolved splitting in six equidistant components for the cubic AN emission at 5 T for **B**‖[111]. The components are marked, starting from the high-energy side with lowered indices. At all magnetic fields the splittings between the components are equidistant and very precise, increasing linearly with the magnetic field. The large sixfold equidistant splitting allowed us to determine the observed g factor with a high accuracy to

$$g = 2.026 \pm 0.010 .$$

With increasing magnetic field only the high-energy component AN_I becomes stronger in intensity while all other components are decreasing. Thus, the weak low-energy component AN_{VI} could only be traced up to 6 T. This effect is certainly not due to thermalization of the excited term, as in this case the low-energy component AN_{VI} should show increasing, and the component AN_I decreasing intensities. This is also in accordance with measurements at higher temperatures ($T = 10$ K) showing the same intensity ratios of the somewhat weaker and broader components. At higher temperatures new emission lines also appeared which will be discussed later.

Figure 6 shows the splitting pattern of the whole zero-phonon line region for the orientation **B**‖[111]. All emissions split nearly identically with the AN emission, although only for the emissions AN, PN, and AS could all six components be resolved. For the other emission lines, at least the low-energy components X_{VI} are covered by much more intense components of other emission lines. All emissions in the zero-phonon region seem to terminate in the same ground state and thus, at $T = 1.8$ K, should be connected with the same electronic transition. The interpretation as zero-phonon lines for most of the emission lines may be wrong, but this seems to be unlikely because of the otherwise required small phonon ener-

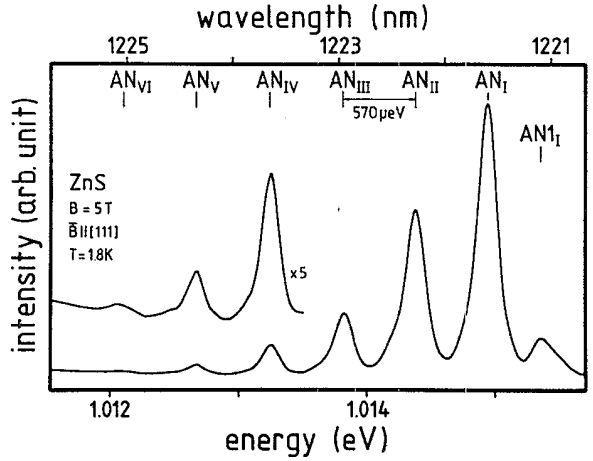

FIG. 5. The AN emission spectrum at $B = 5$ T for the magnetic field orientation **B**‖[111].

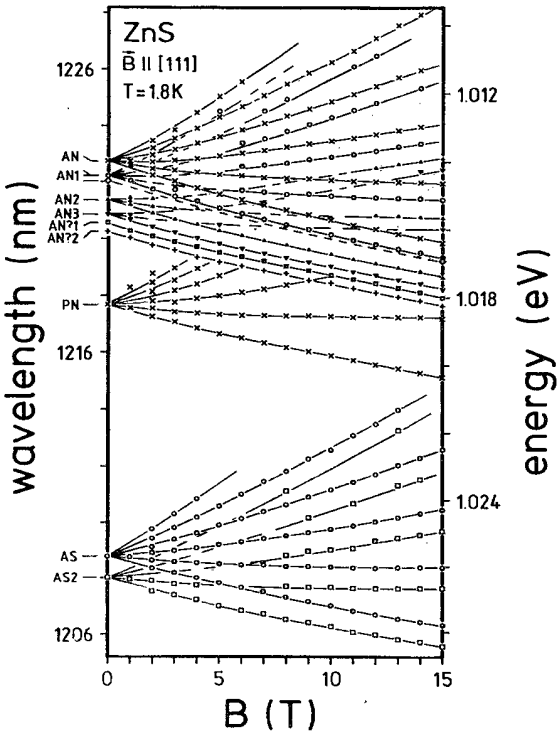

FIG. 6. Zeeman pattern of the whole zero-phonon line region for the magnetic field orientation **B**‖[111].

gies and the observed small linewidths. Furthermore, the energy differences between the centers of gravity of the sixfold splittings of the particular emissions vary with the magnetic field (see Fig. 7) and there is no reason why phonon energies should shift in a magnetic field. The investigation of the phonon sidebands indeed showed that the phonon energies do not change. More probably, the zero-phonon lines originate from the same electronic transitions of slightly different luminescence centers. The polytypic structure of the investigated crystals offer a reasonable probability of such different Zn^{2+} lattice sites.

There are some further results connected with the magneto-optical measurements which should be noted. The orientation of the crystals in the magnetic field have no effect on the line positions in the margin of error but changes the intensity ratios of the components. Thus we are justified in restricting the discussion of the energy positions to the orientation $\mathbf{B}\|[111]$. We do not observe any noticeable polarization effects.

The excitation spectrum of the new luminescence (marked with a question mark) together with that of the $Cu^{2+}(^2E(D)\text{-}^2T_2(D))$ luminescence is shown in Fig. 8, both measured on the same crystal. The excitation spectrum of the new luminescence shows a low-energy threshold near 1.3 eV and a broad structureless band in the visible spectral region with two maxima near 2.42 and 2.83 eV. Such a broad excitation band is rather typical for a charge-transfer excitation band as can be compared with the known visible excitation spectra of the $Cu^{2+}(^2E(D)\text{-}^2T_2(D))$ luminescence (Fig. 8). The near-band-gap excitation could not be detected because the background below the new luminescence becomes comparatively intensive. Emission spectra recorded under near-band-gap excitation (i.e., 365 nm) show the same shape as reported by Godlewski *et al.*[10] for ZnS:Cu,Fe crystals [his Fig. 1(b)]; the new luminescence is not excited.

Below 1.3 eV we did not observe any excitation of the new luminescence due to lack of absorption, although the

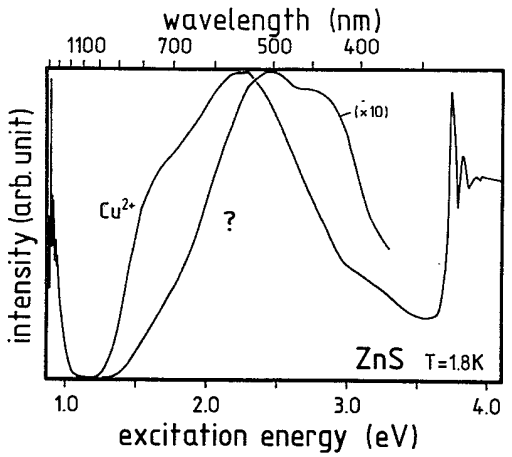

FIG. 8. Excitation spectra of the new (?) and the $Cu^{2+}(^2E(D)\text{-}^2T_2(D))$ luminescence bands in ZnS. Both spectra have been measured on the same crystal.

excitation spectroscopy is much more sensitive than the absorption spectroscopy. The agreement between the low-energy threshold of the new luminescence excitation with that of the charge-transfer band of the $Cu^{2+}(^2E(D)\text{-}^2T_2(D))$ luminescence is remarkable, as can be seen from Fig. 8.

The excitation of the luminescence below 1.3 eV could be stimulated, however, by the additional unmodulated irradiation with 632.8 nm (HeNe laser, 1.959 eV, 0.5 mW). Figure 9 displays the near-infrared spectral region of the excitation spectrum with (b) and without (a) stimulation. We did not observe any fine structures, but checked with corresponding emission measurements that the stimulated excitation really results in the new luminescence. Unfortunately, the signal was too weak for a measurement of the stimulation spectrum. The stimu-

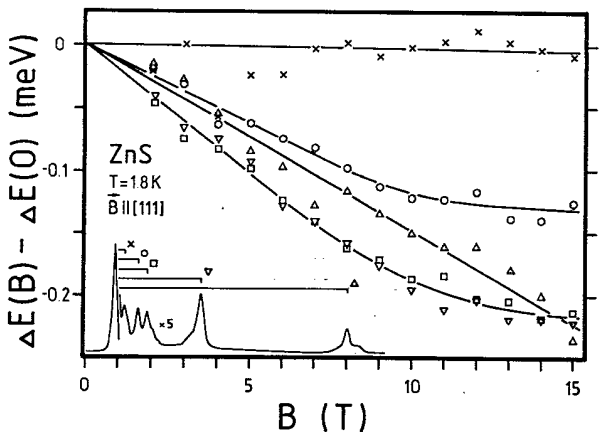

FIG. 7. The variations of the energy differences between the centers of gravity of the different sixfold splittings (Fig. 6) in dependence of the magnetic field ($T = 1.8$ K).

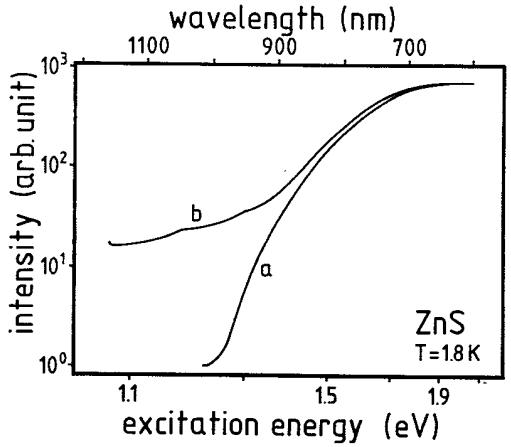

FIG. 9. Excitation spectra of the new luminescence in ZnS (a) without and (b) with stimulation by the additional irradiation with light of the 632.8-nm emission of a He-Ne laser (1.959 eV, 0.5 mW).

lation decays with a time constant of several seconds after the shutoff of the HeNe laser under the continuous excitation with light below and above 1.3 eV. In addition, the stimulation with the weak HeNe laser clearly shows a saturation effect. This demonstrates that the luminescence centers usually have the wrong charge state in the unexcited crystal, but are recharged under irradiation with photon energies above 1.3 eV. Thus, the low-energy region of the excitation spectrum must be dominated by a charge-transfer process either direct or indirect by the capture of free carriers from elsewhere. The slow decay of the stimulation under near-infrared excitation in the range of several seconds shows that the subsequent excitation process of the new luminescence competes with a recharging process of the luminescence center of lower probability.

Up to now we have discussed only emissions originating from the lowest fine-structure state of the excited term, since only this state is noticeably populated at $T=1.8$ K, thus there is no information about the excited states. Information about the fine structures of the excited terms can, in principle, be obtained from the absorption measurements at $T=1.8$ K, but unfortunately we have not been able to detect a measureable absorption. Therefore emission measurements with crystal temperatures higher than 1.8 K were performed. Figure 10 shows the zero-phonon line region of the new luminescence at three different crystal temperatures. The rise in temperature results in the appearance of several additional emission lines, together with a decrease in intensity and broadening of the emission lines, which lead to complicated overlapping spectra which are difficult to interpret. The new emissions arise from thermally populated states of the different centers and reflect the fine structures of their excited terms. Thus, we must connect the new emissions at higher temperatures to those at $T=1.8$ K. This is possible in the cases of the emissions AN, AS, and AS2 for which we observe, respectively, one new line on the high-energy side corresponding to splittings of the excited terms in two states with separations of 0.58, 0.48, and 0.77 meV, respectively. In the case of the PN emission, we observed three new emissions corresponding to a splitting of the excited term in four states with energy separations of 0.86, 1.72, and 2.75 meV to the lowest state. Furthermore, new emission lines are attached to the AN subcenters, but their identification is only tentative. The splitting of the excited terms of the different centers are summarized in Table I.

Figure 11 shows the spectral region of the AN emissions at 14 T and $\mathbf{B}\|[111]$ for two different crystal temperatures (2 and 10 K). The new strong emissions are

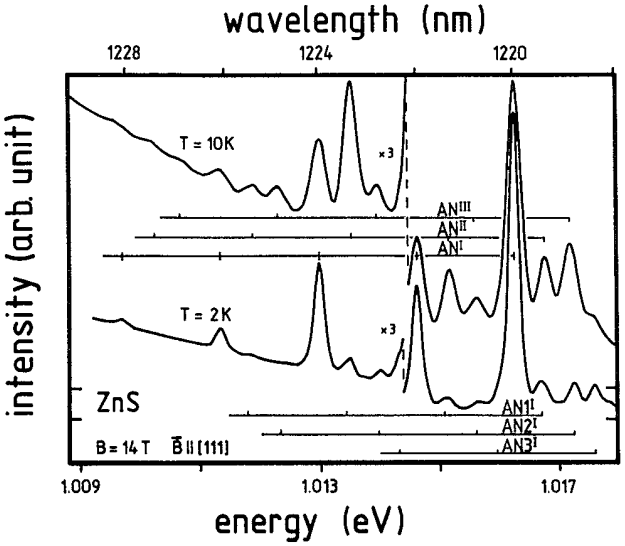

FIG. 11. Luminescence spectrum of a polytypic ZnS crystal in the energy region of the AN emission at $B=14$ T and $\mathbf{B}\|[111]$ for different crystal temperatures (488-nm excitation).

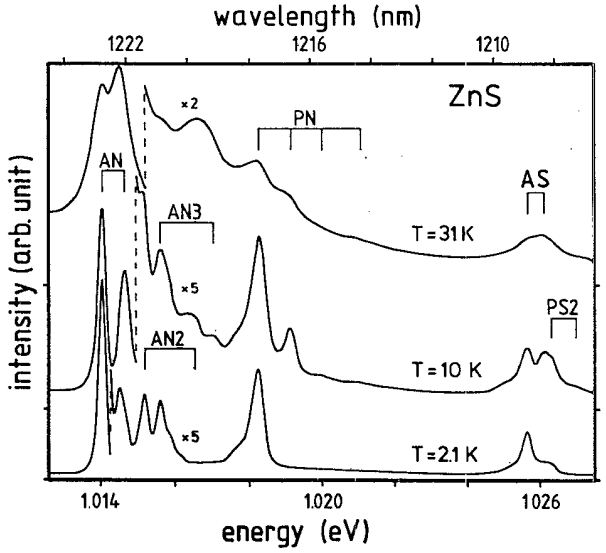

FIG. 10. Luminescence spectra of a polytypic ZnS crystal in the zero-phonon line region of the new luminescence for different crystal temperatures (488-nm excitation).

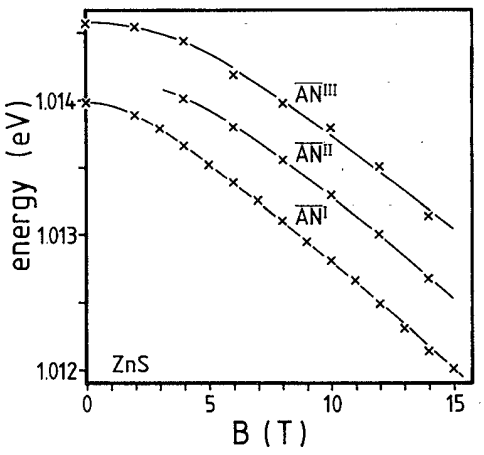

FIG. 12. Zeeman splitting of the excited term of the AN center for the magnetic field configuration $\mathbf{B}\|[111]$.

due to the AN center and do not correspond to the weak lines observed at $T=2$ K. Figure 12 shows the observed splitting of the excited term of the AN center in a magnetic field for $\mathbf{B}\|[111]$, whereby the center of gravity of the sixfold splittings of the $^6A_1(S)$ ground state has been set to zero. We observed at magnetic fields greater than 4 T three components. The two outer originate from the two zero field states, whereas the origin of the central one is not clear.

IV. DISCUSSION

Up to now, many mostly structureless emissions in the near-infrared spectral region have been reported for ZnS, but only two are possible candidates for the new luminescence. Grebe *et al.*[11] reported in 1974 a luminescence band in the 1.2-μm spectral region of a ZnS:Cr crystal. The observed fine structures with one zero-phonon line at 1.0132 eV agree with those of the new luminescence but have worse resolution. The energy position of the luminescence led Grebe to conjecture that perhaps a color center (F^+ center) is the origin. Lepnev *et al.*[12] reported in 1982 a structureless luminescence band (IR-II) with its maximum at 1.27 μm at $T=80$ K for "high-purity" ZnS crystals. The observed visible excitation band with two maxima at 2.9 and 2.3 eV corresponds to the excitation spectrum of our new luminescence structure showing the correspondence of both emissions. Lepnev guessed that it was an intrinsic defect. No further interpretation could be found in the literature.

In order to explain our experimental results we limit the choice of possible centers and make one basic assumption—we assume that the new luminescence is connected with a *d-d* transition of a 3*d* element. The static crystal-field theory describes well the general structures of the d^N configurations on cation sites in II-VI compound semiconductors and predicts their ground states. The magneto-optical measurements have clearly shown that the ground state of the new luminescence has no fine structure ($\Delta E<90$ μeV) and splits in a magnetic field linearly with $g=2.026\pm0.010$ to six equidistant components. The lack of fine structure indicates a term without any orbital angular momentum—an A_1 or A_2 term in T_d symmetry. The lack of an orbital angular momentum is also consistent with the observed g factor, which is close to the free-electron value, indicating a pure spin momentum. In T_d symmetry only for $N=2$, 5, and 7, the d^N configurations have an A_1 or A_2 ground-state term with total spins of 1, $\frac{3}{2}$, and $\frac{5}{2}$, respectively. Since only the $^6A_1(S)$ ground state of the d^5 configuration offers the sixfold degeneracy, the magneto-optical results give clear evidence of a d^5 configuration of the new luminescence center (see Fig. 13).

All excited crystal-field states of the d^5 configuration are spin quartets or doublets, so all electric-dipole transitions to the sextet $^6A_1(S)$ ground state are spin forbidden, consistent with the observed long decay time in the ms range. Therefore, since all recombination processes of the excited d^5 configurations include the energetic lowest quartet term, only the $^4T_1(G)$-$^6A_1(S)$ luminescence can be expected. As we propose a transition metal of the iron

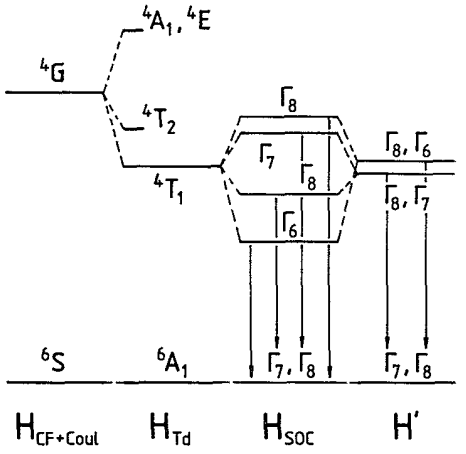

FIG. 13. Term scheme of a d^5 crystal-field configuration.

group as luminescence center, there are only three possible candidates, Cr^+, Mn^{2+}, and Fe^{3+}, known from ESR measurements to substitute Zn^{2+} lattice sites. The three transition metals are incorporated usually in the isoelectronic charge state. The g factors of the $^6A_1(S)$ ground states of the three metals are well known from ESR experiments,[26] whereas information on the excited terms exists only in the case of Mn^{2+}.[27] The yellow $Mn^{2+}(^4T_1(G)$-$^6A_1(S))$ crystal-field luminescence in ZnS starts with a zero-phonon line at 2.218 eV, much too high for the new luminescence. The observed g factor of 2.026 ± 0.010 lies within the margin of error for Fe^{3+}, $g=2.0194$. However, the g factor of Cr^+ (1.9995) is only 1% smaller, not far out of the margin of error. Thus, the observed g factor does not determine definitely whether Fe^{3+} or Cr^+ is the material in question.

In order to identify the new luminescence, we doped ZnS crystals with iron and chromium, respectively. Since we observed sometimes a strong increase in intensity by the temper procedure alone, we cleaved the samples and performed on all fragments the same temper procedure with different additional impurity concentrations. Figure 14 shows the increase of the emission intensity by iron doping, fragment *B* has been doped with iron, whereas fragment *D* has been only tempered. Despite the increase of the total intensity by a factor of 4 to 5, the intensities of the polytypic emission lines increase faster than that of the cubic lines, showing that the crystal structure changes by the doping procedure. Despite the problems connected with the temper procedure, the doping experiments show a clear relation between the iron concentration and the luminescence intensity. This is not the case for the chromium dopings, where such an effect could not be observed. Nevertheless, uncertainty is left from these doping experiments and additional arguments that Fe^{3+} is the center for the new luminescence should be found.

In Sec. III we outlined that the new luminescence centers can only arise in the d^5 charge state under the influence of the exciting light. This is also in accordance with photo-ESR measurements, where the energy thresh-

olds of the direct charge-transfer processes of Cr^+ (Refs. 27 and 28) and Fe^{3+} (Ref. 8) have been determined. Starting from the isoelectronic charge states, the direct charge-transfer reactions

$$Cr^{2+} \xrightarrow{h\nu} Cr^{+} + h_{VB}$$

and

$$Fe^{2+} \xrightarrow{h\nu} Fe^{3+} + e_{CB}$$

produce Cr^+ and Fe^{3+} at photon energies above 2.4 and 2.1 eV, respectively. Both energies are much too high for the observed energy threshold at 1.3 eV. This means the production of the luminescence center in the right d^5 charge state must be connected with an energy transfer by the capture of otherwise freed carriers, by valence-band holes in the case of Fe^{3+} or conduction-band electrons in the case of Cr^+ The determination of the source of these free carriers should allow us to decide between Cr^+ and Fe^{3+} as the luminescence center. The only reasonable carrier source in this spectral region is Cu^{2+}, which is a quite normal contamination in our crystals. The charge-transfer process

$$Cu^{2+}(^2T_2(D)) \xrightarrow{h\nu} Cu^{+} + h_{VB}$$

is connected with the broad visible excitation band of the $Cu^{2+}(^2E(D)$-$^2T_2(D))$ luminescence. The low-energy threshold of this band agrees well with that of the new luminescence. Therefore we propose that the capture of valence-band holes is responsible for the charge transfer of the new luminescence centers. From this the luminescence center can only be attributed to the Fe^{3+} ion. A detailed study of the energy transfer process between Cu^{2+} and Fe^{2+} centers by free holes which lead to a more detailed understanding of the system ZnS:Cu^{2+} will be given elsewhere.[29]

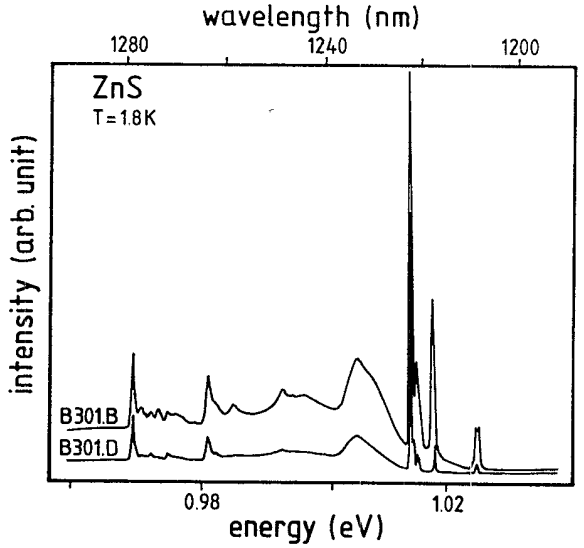

FIG. 14. Luminescence spectra in the energy region of the new luminescence of the polytypic ZnS crystal $B301$. Fragment B has been intentionally doped with iron by vapor deposition and subsequent diffusion at 1040 °C for 40 h. Fragment D has been only tempered at 1040 °C for 40 h.

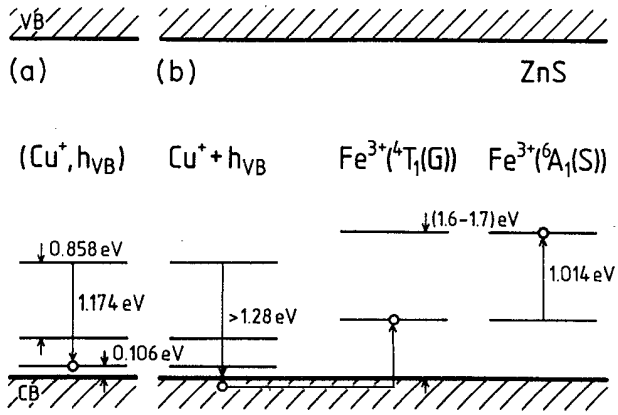

FIG. 15. Schematic hole picture of the excitation processes of the Fe^{3+} luminescence. (a) Creation of the (Cu^+,h_{VB}) complexes (Ref. 29) for excitation energies between 1.174 and 1.28 eV. (b) Creation of free holes for excitation energies greater than 1.28 eV and their capture through the Fe^{2+} center.

The broad visible excitation band of the new Fe^{3+} luminescence in the energy region above 1.7 eV agrees well with the charge-transfer band

$$Fe^{3+}(^6A_1(S)) \xrightarrow{h\nu} Fe^{2+}(^5E(D)) + h_{VB}$$

as it has been observed by Zimmermann[30] in photoinduced absorption measurements at $T=80$ K on ZnS:Fe crystals. Additionally, the appearance of this charge-transfer band in the excitation spectrum of the $Fe^{3+}(^4T_1(G)$-$^6A_1(S))$ luminescence shows an effective energy transfer from the valence band to the excited Fe^{3+} terms. Subsequently, the Fe^{3+} relaxes radiatively with the emission of the detected near-infrared luminescence (see Fig. 15).

The observed excitation spectrum of the $Fe^{3+}(^4T_1(G)$-$^6A_1(S))$ luminescence can roughly be divided into two different spectral regions which differ by the reexcitation process subsequent to the hole capture process mentioned above. In the energy range between 1.3 and 1.7 eV no direct recharging of the Fe^{3+} centers is possible. Therefore, the Fe^{3+} center is excited only by its own crystal-field absorption. This is shown in Fig. 9, where the Fe^{3+} is steadily created by a He-Ne laser source. A different reexcitation process takes place in the region above 1.7 eV, where the direct recharging of the Fe^{3+} ions dominates the crystal-field absorptions and leads to the observed charge-transfer band:

$$
\begin{aligned}
Cu^{2+}(^2T_2(D))+Fe^{2+}(^5E(D)) &\xrightarrow{h\nu} Cu^{+}+h_{VB}+Fe^{2+}(^5E(D)) \quad (h\nu>1.3\ \text{eV})\\
&\longrightarrow Cu^{+}+Fe^{3+}(^4T_1(G))\\
&\longrightarrow Cu^{+}+Fe^{3+}(^6A_1(S))+h\nu_{IR}\\
\text{(I)}\xrightarrow{h\nu}\ & Cu^{+}+Fe^{3+}(^4T_1(G)) \quad (h\nu<1.7\ \text{eV})\\
\text{either}\longrightarrow\ & Cu^{+}+Fe^{3+}(^6A_1(S))+h\nu_{IR}\\
\text{or}\xrightarrow{h\nu}\ & Cu^{+}+h_{VB}+Fe^{2+}(^5E(D)) \quad \text{(two step)}\\
\text{(II)}\xrightarrow{h\nu}\ & Cu^{+}+h_{VB}+Fe^{2+}(^5E(D)) \quad (h\nu>1.7\ \text{eV})\ .
\end{aligned}
$$

Georgiobani[13] investigated the behavior of his IR-II luminescence in time-resolved two-beam experiments. The spectrum obtained coincides with the stimulated excitation spectra of the $Fe^{3+}(^4T_1(G)$-$^6A(S))$ luminescence.

Having established the general origin of the Fe luminescence we have to explain the fine structure. At $T=1.8$ K only one zero-phonon emission can be expected for the $^4T_1(G)$-$^6A_1(S)$ luminescence of an Fe^{3+} center in T_d symmetry due to the thermalized $^4T_1(G)$ term and the total degenerated $^6A_1(S)$ term. Therefore, the observed zero-phonon lines must be connected with slightly different luminescence centers, as has been outlined above. Since the chemical nature of all centers is obviously the same, the Zn^{2+} lattice sites cannot be equivalent. The investigated ZnS crystals were preferably cubic but also contained stacking faults. The arrangements of the nearest neighbors from Zn^{2+} lattice sites differ according to their relative position to such stacking faults. Out of optical spectra of other $3d$ elements it is well known that these distortions from the cubic arrangement result in slightly shifted and partly split energy levels. If one considers only the possible arrangements of the three nearest neighbors, one obtains four different centers called AN (cubic), PN, AS, and PS (hexagonal), as described in more detail in the frame of the polytypic point defects.[31,32]

As the isoelectronic Mn^{2+} has been investigated and interpreted in the framework of the distorted cubic crystal structure,[31] we will interpret the fine structure of the Fe^{3+} luminescence according to that of the Mn^{2+} luminescence. This means the group of emissions around 1.015 eV is due to the AN centers, the emissions at 1.018 eV are due to the PN centers, and the emissions around 1.026 eV are due to the AS centers. The identification of the PN center is confirmed by the observed fourfold splitting of the $^4T_1(G)$ term which coincides with the observed fine structure of the Mn^{2+} PN center. The intensive emission at 1.013 99 eV is due to the pure cubic AN center. In Fig. 3 the emissions are marked by their proposed luminescence centers. The observed Fe luminescence is the superposition of the luminscence structures from at least 9 different Fe^{3+} centers.

All polytypic centers, except the cubic AN center, are connected with an axial axis, the $(111)_{growth}$ axis of the cubic crystal. The symmetry reduction connected with the axial crystal-field part normally leads to polarized dipole transitions. Therefore, at first sight, it is not clear why no polarization effects have been observed for the $^4T_1(G)$-$^6A_1(S)$ transitions of polytypic Fe^{3+} and Mn^{2+} centers in ZnS. The reason can be found in the vanishing influence of the c_{3v} crystal-field part. No corresponding splittings of the fine structure of the $^4T_1(G)$ and $^6A_1(S)$ terms have been observed in the optical spectra. The energy shifts in the polytypic centers are due to changes in the cubic crystal-field parameters. Also, in a magnetic field, each state of the $^4T_1(G)$ term has a residual threefold degeneracy due to the strong Jahn-Teller coupling to E modes. The remaining degeneracy can explain the lack of noticeable polarizations.

The fine structure of the $^6A_1(S)$ ground terms of various Fe^{3+} centers in II-VI compounds are well known from ESR measurements. In general, a reduction of the point symmetry from T_d to c_{3v} lifts the sixfold degeneracy by a splitting in three Kramers doublets, whereby the total splitting is found to lie normally below 100 μeV. Buch *et al.*[33] observed ESR signals of Fe^{3+} on different axial sites in polytypic ZnS crystals (AS and PN centers) and found the g value of the cubic center and total zero-field splittings in the range of 35 μeV due to the trigonal part of the crystal field. These zero-field splittings are well covered by the inhomogeneous linewidths of the optical zero-phonon lines in the range over 210 μeV, nevertheless they can explain the smaller inhomogeneous linewidth of the cubic AN emission of 180 μeV. The zero-field splittings of the $^6A_1(S)$ ground states of the axial centers also result in deviations from the equidistant Zeeman splittings in the same size, which also lie in the margin of experimental error. Iron in II-VI compounds is known to form associates with other point defects. These associates are connected with much larger axial distortions from the cubic crystal field. For ZnS, Holton *et al.*[34] determined the total splittings of the $^6A_1(S)$ ground states of Fe^{3+} in Fe-Ag and Fe-Cu complexes to be 245 and 631 μeV, respectively, which are much too large to be covered by the inhomogeneous linewidths or the experimental error. Thus, we deal with isolated Fe^{3+} centers.

The static crystal-field theory (see Fig. 13) predicts a fourfold splitting of the $^4T_1(G)$ term by the spin-orbit interaction in the range of 10 meV, in contrast to the observed fine structure of the $^4T_1(G)$ terms of the different Fe^{3+} centers. Only for the PN center did we observe a fourfold splitting of the $^4T_1(G)$ term, but the overall splitting of 2.75 meV is much too small, whereas at the other centers only twofold splittings were found. The different Mn^{2+} centers in polytypic ZnS crystals exhibit the same behavior, which has been explained by a strong Jahn-Teller effect.[35] A strong coupling of the $^4T_1(G)$ term to E modes results in a reduction of the spin-orbit

splitting, leading to a residual second-order splitting in two states. The observed fourfold fine structure of the $^4T_1(G)$ term from the PN center corresponds to a weaker Jahn-Teller coupling, also observed for the PN center of Mn^{2+}.

Fournier *et al.*[36] calculated the magnetic field dependence of the $^4T_1(G)$ term of Mn^{2+} under the assumption of a strong Jahn-Teller coupling to E modes. He found an agreement with the experimental results of a fourfold splitting of the two states in a magnetic field orientation $\mathbf{B}\|[111]$. In the framework of his calculation, we must suppose that the central component in Fig. 12 consists either of two components originating from the two zero-field states or originates from the energetic lower state. A comparison of the observed intensity ratios with those observed and calculated for ZnS:Mn favors the latter assumption. Fournier investigated the excitation spectrum of the $^4T_1(G)$-$^6A_1(S)$ luminescence at $T=1.1$ K, so one has to compare his intensities with those observed for the components AN_1^I, AN_1^{II}, and AN_1^{III} in Fig. 11 at 10 K. The intensity ratios are nearly the same if one takes into consideration the thermalization of the $^4T_1(G)$ term at $T=10$ K. This means we have not observed the weak high-energy component due to the additional polytypic emissions. Therefore, the observed fine structure and magnetic field behavior of the excited term of the Fe^{3+} luminescence confirms the identification as a $^4T_1(G)$ term and is consistent with a similar Jahn-Teller coupling to E modes, as has been observed for ZnS:Mn. Further information is needed for a detailed analysis of the $^4T_1(G)$ terms of the Fe^{3+} centers in polytypic ZnS crystals, which may be obtained in improved absorption or excitation measurements.

The small energy of the $^4T_1(G)$-$^6A_1(S)$ transition of Fe^{3+} compared to Mn^{2+} in ZnS cannot be explained in a simple crystal-field treatment. The energy corresponding to the energy difference ^6S-^4G of the free Fe^{3+}-ion amounts to 4.07 eV.[37] A strong covalent reduction in electron repulsion, which lowers the energies of all states, can be observed for all crystal-field environments, e.g., the small transition energies of $FeCl_4^-$ indicate a 44% reduction.[37,38] For the Fe-S center in rebredoxin the $^4T_1(G)$-$^6A_1(S)$ transition has an energy of 0.89 eV corresponding to a covalent reduction of 65%.[38] For ZnS:Fe^{3+}, discussed in this paper, it is known that two effects lower the $^4T_1(G)$ energy level: a strong reduction of the Racah parameter B by the covalent binding to the S ligands and a stronger crystal-field parameter Dq for Fe^{3+} than for Mn^{2+}.

V. CONCLUSION

In high-purity ZnS crystals we observed a richly structured luminescence centered near 1.0 eV. The general appearance of this luminescence indicates a quite common "intrinsic" defect, such as transition elements of the iron group which are normally present in the ppm range. The observed shape indicates also a *d-d* transition. The behavior of the zero-phonon lines in a magnetic field revealed a sixfold-degenerate ground state for all emissions, with an isotropic g factor of 2.026 ± 0.010. Such a ground state is consistent with the $^6A_1(S)$ ground state of a d^5 configuration. Mn^{2+} is well known for its yellow emission and can be excluded for energetic reasons. The choice between the two remaining candidates Cr^+ and Fe^{3+} has been made possible by intentional Fe doping and by the observed excitation behavior, which is dominated by a charge-transfer process whereby the luminescence center arises in the needed charge state. The low-energy threshold near 1.3 eV cannot be explained by Cr nor Fe centers, but corresponds well to the photoionization energy of Cu^{2+}. Therefore, the observed charge transfer of the luminescence centers has been explained by an energy transfer by free holes from Cu^{2+} centers, consistent with Fe^{3+} as luminescence center. Due to the spin-selection rules, only the $^4T_1(G)$-$^6A_1(S)$ luminescence can be expected. This transition also explains the observed long decay time in the ms range.

By a comparison with the well-studied $^4T_1(G)$-$^6A_1(S)$ transitions of the isoelectronic Mn^{2+} centers, we have shown that the similarities with the observed fine structures persits. The numerous zero-phonon lines at $T=1.8$ K could be assigned to isolated Fe^{3+} centers in different distorted cubic surroundings; the transition of the pure cubic AN center lies at 1.013 99 eV. The fine structures of the $^4T_1(G)$ terms, observable at higher temperatures, are the analogy to those of the corresponding Mn^{2+} centers, indicating the same strong Jahn-Teller coupling to E modes for the Fe^{3+} centers.

From the investigation of the Fe^{3+} centers, one can expect in the future interesting information about the influence of the positive excess charge on the d^5 configuration, e.g., the reduction of the Racah parameter B corresponding to the quenched transition energy. The rearrangement of the charges in the vicinity of the deep charged impurity can be the origin.

ACKNOWLEDGMENTS

This paper has been supported by the Deutsche Forschungsgemeinschaft (Bonn, Germany). The authors wish to thank Dr. R. Broser for supplying the crystals, B. Hausmann for his help during the doping procedure, and H. Perls for technical help with the Zeeman measurements.

[1]R. H. Bube, *Photoconductivity of Solids* (Wiley, New York, 1960).
[2]H. A. Weakleam, J. Chem. Phys. **36**, 2117 (1962).
[3]J. W. Allen, J. Phys. **2**, 1077 (1969).
[4]J. M. Langer and H. Heinrich, Phys. Rev. Lett. **55**, 1414 (1985).
[5]W. Hoogenstraaten and H. A. Klasens, J. Electrochem. Soc. **100**, 366 (1953).
[6]F. S. Ham and G. A. Slack, Phys. Rev. B **4**, 777 (1971).
[7]K. E. Tarkpea and A. Ots, Phys. Status Solidi B **129**, 799 (1985).
[8]M. Godlewski and Z. Zakrzewski, J. Phys. C **18**, 6615 (1985).
[9]M. Skowronski and Z. Liro, J. Lumin. **24/25**, 253 (1981).
[10]M. Godlewski, W. E. Lamb, and B. C. Cavanett, J. Phys. C **15**, 3925 (1982).

[11]G. Grebe and H.-J. Schulz, Z. Naturforsch. **29a**, 1803 (1974).
[12]L. S. Lepnev and V. F. Tunitskaya, Zh. Prikl. Spektrosk. **36**, 40 (1982).
[13]A. N. Georgiobani, L. S. Lepnev, E. I. Panasynh, and V. S. Tunitskaya, Zh. Prikl. Spektrosk. **42**, 443 (1985).
[14]I. Broser, A. Hoffmann, R. Germer, R. Broser, and E. Birkicht, Phys. Rev. B **33**, 8196 (1986).
[15]I. Broser, H. Maier, and H.-J. Schulz, Phys. Rev. **140**, A2135 (1965).
[16]I. Broser and K. H. Franke, J. Phys. Chem. Solids **26**, 1013 (1965).
[17]I. Broser, R. Broser, and E. Birkicht, J. Lumin. **31/32**, 424 (1984).
[18]G. Roussos and H.-J. Schulz, Solid State Commun. **51**, 663 (1984).
[19]I. Broser, R. Germer, F. Seliger, and H.-J. Schulz, J. Phys. Chem. Solids **41**, 101 (1980).
[20]A. Hoffmann, I. Broser, and P. Thomsen-Schmidt, J. Lumin. **40/41**, 321 (1988).
[21]A. Hoffmann, R. Heitz, and I. Broser (unpublished).
[22]G. A. Slack and S. Roberts, Phys. Rev. B **3**, 2613 (1971).
[23]D. N. Talwar and Bal. K. Agrawal, Phys. Status Solidi B **64**, 71 (1974).
[24]A. Memon and D. B. Tanner, Phys. Status Solidi B **127**, 49 (1985).
[25]M. Zigone, M. Vandevyver, and D. N. Talwar, Phys. Rev. B **24**, 5763 (1981).
[26]R. S. Title, Phys. Rev. **131**, B623 (1963).
[27]M. Godlewski and M. Kaminska, J. Phys. C **13**, 6537 (1980).
[28]M. Godlewski, Z. Wilamowski, M. Kaminska, W. E. Lamb, and B. C. Cavenett, J. Phys. C **14**, 2835 (1981).
[29]A. Hoffmann, R. Heitz, and I. Broser (unpublished).
[30]H. Zimmermann, R. Boyn, and N. Nagel, Phys. Status Solidi B **117**, 229 (1983).
[31]W. Busse, H.-E. Gumlich, W. Knaak, and J. Schulz, J. Phys. Soc. Jpn. **49**, Suppl. A581 (1980).
[32]U. W. Pohl, H.-E. Gumlich, and W. Busse, Phys. Status Solidi B **125**, 773 (1984).
[33]T. Buch, B. Clerjaud, B. Lambert, and P. Kovacs, Phys. Rev. B **7**, 184 (1973).
[34]W. C. Holton, M. De Wit, T. L. Estle, B. Dischler, and J. Schneider, Phys. Rev. **169**, B359 (1968).
[35]P. Koidl, Phys. Status Solidi B **74**, 477 (1976).
[36]D. Fournier, A. C. Boccara, and J. C. Rivoal, J. Phys. C **10**, 113 (1977).
[37]C. K. Jörgenson, Discuss. Faraday Soc. **26**, 110 (1958).
[38]J. C. Deaton, M. S. Gebhard, S. A. Koch, M. Millar, and E. I. Solomon, J. Am. Chem. Soc. **110**, 6241 (1988).